Chiang Mai J. Sci. 2016; 43(2) : 345-350
http://epg.science.cmu.ac.th/ejournal/
Contributed Paper

# Synthesis and Characterization of Cubic-like Zinc Stannate Powders Prepared by Co-precipitation Method

**Wanichaya Mekprasart, Thanit Tangcharoen, Puritat Nakhanivej and Wisanu Pecharapa***
College of Nanotechnology, King Mongkut's Institute of Technology Ladkrabang (KMITL), Bangkok, 10520, Thailand.
*Author for correspondence; e-mail: kpewisan@gmail.com

Received: 15 September 2015
Accepted: 12 November 2015

## ABSTRACT

Spinel-type zinc stannate ($Zn_2SnO_4$) powders were synthesized by co-precipitation method using zinc chloride and tin chloride as the precursors for Zn and Sn sources, respectively. Co-precipitation process is one of effective techniques due to non-complex system, short process time, high yield, large scale production and cost-effectiveness comparing to other methods. The influence of calcination temperature in the range of 900 °C to 1100 °C on the structure, morphologies and cation distribution were studied using various characterization techniques. A single spinel structure phase formation after-calcined powders are confirmed by X-ray diffraction (XRD) results meanwhile scanning electron microscope (SEM) showed the appearance of cubic-like shape. The aggregation of particle and strong crystallinity was distinctly increased resulting to their greater size by the effect of high calcined temperature. Moreover, the non-equilibrium site occupancy of zinc ($Zn^{2+}$) and tin ($Sn^{4+}$) ions was investigated through Zn *K*-edge and Sn *L3*-edge investigated by X-ray absorption (XAS) spectra via the synchrotron radiation light source. Compared with the calcined temperature sample, XANES spectra revealed that the oxidation state of Zn was +2 and Sn valence was +4 in all spinel $Zn_2SnO_4$ samples which well corresponds to the theoretical values.

**Keywords:** Calcination, Co-precipitation, Cube-like structure, $Zn_2SnO_4$

## 1. INTRODUCTION

The ternary semiconducting oxide spinel-type zinc stannate, $Zn_2SnO_4$, is an important member of stannate family. Interest in this kind of oxide has greatly increased in the last decade because of its fascinating properties in photocatalytic activity, high electrical conductivity and low visible absorption [1]. Generally, $Zn_2SnO_4$ is n-type semiconductor with wide band gap of 3.6 eV and electron mobility of 10-15 $cm^2\ V^{-1}\ s^{-1}$ [2]. In the bulk state, $Zn_2SnO_4$ is stable in the totally inverse spinel structure, which $Zn^{2+}$ cations occupy in both tetrahedral (*A*) and octahedral (*B*) sites meanwhile $Sn^{4+}$ cations occupy in octahedral (*B*) sites [3, 4]. To describe the cations distribution, the structural formula of spinel

can be written as $(Zn^{2+})$ $[Sn^{4+}Zn^{2+}]$ $O_4$, where parentheses and square bracket are assigned to *A* and *B*-sites, respectively. According to the $Zn_2SnO_4$ properties, it can be applied in many fields of applications such as gas sensor, synergistic flame retardants, dye-sensitized solar cell, luminescence materials, anode electrode for Li-ion batteries, and degradation of organic pollutant [5-10].

To obtain $Zn_2SnO_4$, many techniques have been proposed to synthesize this kind of oxide powders such as hydrothermal, spray pyrolysis, solid state reaction, supercritical water in a batch reactor, and mechano-chemical grinding method [11-15]. Stambolova *et al.* [15] reported that $Zn_2SnO_4$ could be obtained by thermal decomposition of zinc hydroxystannate, $ZnSn(OH)_6$, at the temperature above 900 °C. Wang *et al.* [16] doped $Dy^{3+}$ ion into $Zn_2SnO_4$ spheres by co-precipitation method and investigated the photoluminescence and photocatalytic properties of their products. Ali *et al.* [1] studied the effect of mineralizer concentration, hydrothermal temperature, solvent composition, and kind of amines in the simple hydrothermal system on the structural, surface morphology, optical, and photocatalytic activity properties of $Zn_2SnO_4$ powders. Due to the nanosize, $Zn_2SnO_4$ products could be utilized as photocatalyst in photodegradation of methyl orange and photocatalytic activity for $H_2$ evolution from ethanol aqueous solution. Annamalai *et al.* [17] synthesized $Zn_2SnO_4$ nanoparticles by hydrothermal process using $Na_2Co_3$ as a new mineralizer. The results showed that $Zn_2SnO_4$ products had the particle size in the range of 20 nm to 50 nm, which was considered to be ideal for dye-sensitized solar cell application. Zn-Sn-O compound nanopowders in the ternary ($Zn_2SnO_4$: spinel and $ZnSnO_3$: perovskite) and coupled binary ($ZnO/SnO_2$) forms synthesized via simple solid-state mechanochemical method possessed the highly disordered in each structures were reported by Ivetic *et al.* [18]. From previous mentioned works, co-precipitation method combined with calcination process is one of effective technique due to many advantages including process simplicity, short process time, high yield, large scale of production, and cost-effectiveness. Moreover, the purity structure, uniform and small powders can be carried out by this process. One of the crucial process conditions in this technique is calcination temperature. Therefore, the purpose of this research is to synthesize pure $Zn_2SnO_4$ powders with unique cube-like morphology by simple co-precipitation method combined with calcination process and the influence of calcination temperature on their relevant physical properties is in our focus.

## 2. EXPERIMENTAL DETAILS

All reagents were analytical grade without further purification. Zinc chloride ($ZnCl_2$) (Ajax Finechem) and tin (IV) chloride pentrahydrate ($SnCl_4$-$5H_2O$) (Sigma-Aldrich) were used as the zinc and tin sources, respectively. 0.25M 100 ml of both materials were prepared and mixed under vigorous magnetic stirring. The solution was precipitated in room temperature by added dropwise of 0.5M NaOH until pH value in the system of 14 was reached. After that the white precipitate was washed for several times until pH value approximately equaled to 7, then dried in the oven at 100 °C for 24 h. Finally, dried powders were calcined at 100 °C intervals from 900 °C to 1100 °C from room temperature in air for 7 h to obtain spinel structure. The final products were kept in dry place to avoid the moisture.

Structural properties and phase identification of all samples were characterized

by X-ray diffraction (XRD) using Cu $K_\alpha$ irradiation ($\lambda$ = 1.5406 Å) in the $2\theta$ range of 20° to 80° with a scanning rate of 0.02° $s^{-1}$. Scanning electron microscope (SEM) was used to investigate the surface morphology and microstructure of samples. The thermal property of as-precipitated powders was carried out by thermal gravimetric analysis technique (TGA) in oxygen-nitrogen atmosphere, ranging from 32 °C to 900 °C at heating rate of 10 °C/min. The oxidation state was analyzed through Zn *K*-edge (9659 eV) and Sn *L3*-edge (3929 eV) XANES spectra, measured at room temperature in the transmission mode.

## 3. RESULTS AND DISCUSSION

Figure 1 shows the thermal analysis of as-precipitated powders, $ZnSn(OH)_6$, obtained after drying at 100 °C. One small mass loss can be observed on the TG curve at the temperature about 190 °C to 260 °C (Percent mass loss from the experimental data is 14.34%). The DTG curve exhibits exothermic-endothermic peak at the temperature in the range of the same as mass loss temperature that could be attributed to phase transformation processes from zinc hydroxystannate, $ZnSn(OH)_6$, to perovskite-zinc stannate, $ZnSnO_3$, and the evaporation of water molecules according to equation (1). Mass loss of water molecules from equation (1). was calculated ($M_{loss}$ = 14%) and it was in good agreement to experimental data. At the higher temperature (~600 °C), $ZnSnO_3$ could be transformed to be spinel-zinc stannate, $Zn_2SnO_4$.

$$ZnSn(OH)_{6(s)} + Zn(OH)_{2(s)} \rightarrow ZnSnO_{3(s)} + Zn(OH)_{2(s)} + 3H_2O_{(g)} \quad (1)$$

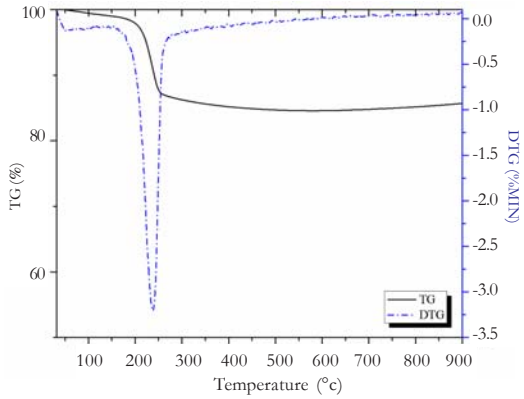


**Figure 1.** TG-DTG curve for as-precipitated powders, $ZnSn(OH)_6$.

Figure 2 shows the XRD patterns of $Zn_2SnO_4$ powders calcined at the different temperatures. For as-prepared sample, XRD pattern is compatible with $ZnSn(OH)_6$ that can be developed by ion exchange between Zn-Sn cations from chloride pre-cursor and $OH^-$ anion from NaOH solution in co-precipitate reaction by following equation (2);

$$2ZnCl_{2(aq)} + SnCl_{4(aq)} + 8NaOH_{(aq)} \rightarrow ZnSn(OH)_{6(s)} + Zn(OH)_{2(s)} + 8NaCl_{(aq)} \quad (2)$$

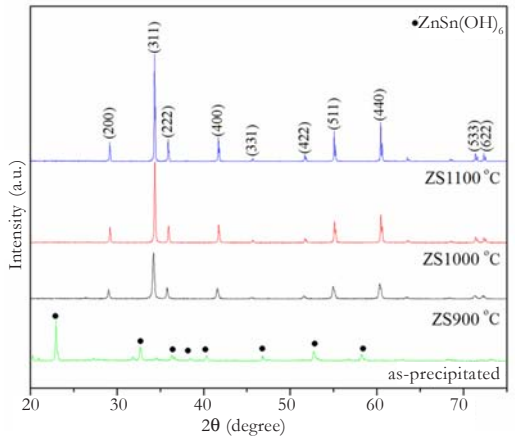


**Figure 2.** XRD patterns of $Zn_2SnO_4$ powders calcined at 900 °C (ZS900), 1000 °C (ZS1000), and 1100 °C (ZS1100).

However, the product of $Zn(OH)_2$ is not detected in XRD pattern due to its naturally amorphous phase. The intermediate product of $ZnSn(OH)_6$ and $Zn(OH)_2$ could be further dehydrated and transformed to stable $Zn_2SnO_4$ phase following this reaction,

$$ZnSn(OH)_{6(s)} + Zn(OH)_{2(s)} \rightarrow Zn_2SnO_{4(s)} + 4H_2O_{(g)} \quad (3)$$

Therefore, calcination process is crucial for the decomposition of as-prepared sample to stable $Zn_2SnO_4$ ternary oxide material. It can be clearly seen that there is no any strange diffraction peak of any impurities in these after-calcined zinc stannate powders but exclusively remain the main diffraction peaks at about 29.2°, 34.4°, 36.0°, 41.7°, 45.7°, 52.5°, 55.2°, 60.5°, 71.6°, and 72.1°, which attribute to the (220), (311), (222), (400), (331), (422), (511), (440), (533) and (622) planes, respectively [7]. This occurrence indicates the completed formation of spinel structure and matches with the JCPDS card no. 74-2184 [1]. The obvious and strong diffraction peaks indicate that these zinc stannate powders exhibit well-formed crystalline structure. However, as calcination temperature increased to 1100 °C, all diffraction peaks are gradually intense and sharpened. This feature is related to the significant increase of the particle size (*D*) from 45 nm for ZS900, to 84 nm for ZS1000, and 109 nm for ZS1100, which were estimated from the broadening of strongest diffraction peak by Scherrer's equation (4). It is noted that *D* is particle size, $\lambda$ is wavelength of X-ray source, $\beta$ is the full width at half-maximum (FWHM) of the (311) diffraction peak, and $\theta$ is its angular position.

$$D = \frac{0.9\lambda}{\beta\cos\theta} \quad (4)$$

Figure 3 shows the morphological characteristics and the microstructures of as-precipitated and after-calcined $Zn_2SnO_4$ powders. For as-precipitated sample (Figure 3a), the formation of micro-cube $ZnSn(OH)_6$ with the agglomeration of $Zn(OH)_2$ amorphous material surrounded on its cube structure was appeared after complete precipitate reaction according to XRD pattern [11]. After the calcination at 900 °C (Figure 3b), it is clearly seen that the finer micro-cube with uniform particle size and homogenous spherical shape were obtained [11]. However, after calcination at more than 1000 °C (Figure 3c and 3d), the aggregation of particle was distinctly increased and made their size greater than the estimated values from the XRD data.

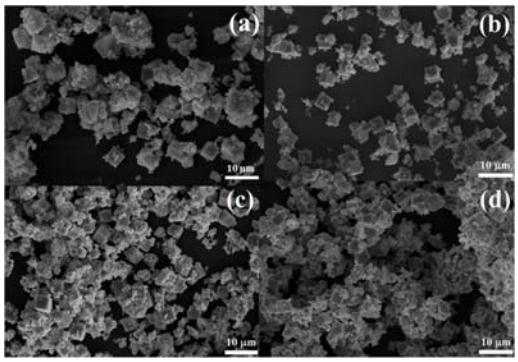


**Figure 3.** SEM photographs of (a) as-precipitated powders and $Zn_2SnO_4$ powders calcined at (b) 900 °C, (c) 1000 °C, and (d) 1100 °C.

Figure 4 shows the experimental XANES spectra of Zn *K*-edge (Figure 4a) and Sn *L3*-edge (Figure 4b) of $Zn_2SnO_4$ powders calcined at 900 °C (ZS900), 1000 °C (ZS1000) and 1100 °C (ZS1100) with ZnO and $SnO_2$ powders as reference standard materials. For Zn *K*-edge and Sn *L3*-edge spectra, it can be clearly seen that the absorption edge energies ($E_0$) of all samples are similar to the standard ZnO (9661.5 eV) and $SnO_2$

(3930 eV), respectively, which confirm the 2+ and 4+ oxidation state of zinc and tin ions for these stannates [19]. Moreover, Sn *L3*-edge XANES spectra shows the same feature presented in the $SnO_2$ spectrum, indicating that $Sn^{4+}$ ions in all samples are probably octahedrally coordinated by 6 oxygen atoms [20].

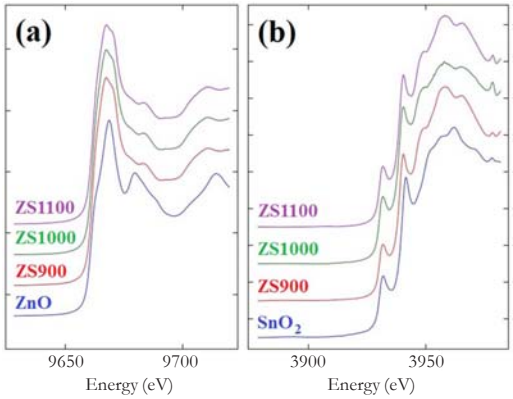


**Figure 4.** Experimental XANES spectra measured at (a) Zn *K*-edge and (b) Sn *L3*-edge of $Zn_2SnO_4$ powders calcined at 900 °C (ZS900), 1000 °C (ZS1000), and 1100 °C (ZS1100) with reference standard materials (ZnO and $SnO_2$).

## 4. CONCLUSION

From this research, cubic-like $Zn_2SnO_4$ powders calcined at different temperatures ranging from 900 °C to 1100 °C were successfully synthesized by co-precipitation method and calcination. XRD results disclose the formation of the single-phase spinel structure for all after-calcined samples. The calculation from diffraction data, including SEM images, reveals that the particle size and shape significantly change with the increase in calcination temperatures. Moreover, XANES spectra present the existence of accurate oxidation state for $Zn^{2+}$ and $Sn^{4+}$ in all spinel system.

## ACKNOWLEDGEMENTS

This work is supported by King Mongkut's Institute of Technology Ladkrabang [KREF045711]. Authors would like to thank KMITL Research Fund, Rajamangala University of Technology Thanyaburi (RMUTT) for XRD measurement, and Beamline 8 (BL8) at Synchrotron Light Research Institute (SLRI), Thailand for XANES measurement.

## REFERENCES

[1] Ali M.B., Bouaifel F.B., Elhouichet H., Sieber B., Addad A., Boussekey L., Férid M. and Boukherroub R., *J. Colloid Interf. Sci.*, 2015; **457**: 360-369.

[2] Sepelak V., Becker S.M., Bergmann I., Indris S., Scheuermann M., Feldhoff A., Kubel C., Bruns M., Sturzl N., Ulrich A.S., Ghafari M., Hahn H., Grey C.P., Becker K.D. and Heitjans P., *J. Mater. Chem.*, 2012; **22**: 3117-3126.

[3] Tangcharoen T., Kongmark C. and Pecharapa W., *J. Molecular Structure*, 2015; **1102**: 95-100.

[4] Kitajou A., Yoshida J., Nakanishi S., Okada S. and Yamaki J., *J. Power Sources*, 2013; **244**: 658-662.

[5] An D., Wang Q., Tong X., Zhou Q., Li Z., Zou Y., Lian X., Li Y., *Sensor. Actuat. B*, 2015; **213**: 155-163.

[6] Petsoma A., Roengsumran S., Ariyaphattanakul A. and Sangvanich P., *Polym. Degrad. Stabil.*, 2003; **80**: 17-22.

[7] Liu M., Yang J., Feng S., Zhu H., Zhang J., Li G. and Peng J., *Mater. Lett.,* 2012; **76**: 215-218.

[8] Park S., Kim S., Choi S., Lee S., Lee C., *Thin Solid Films*, 2015; **591**: 336-340.

[9] Kim K., Annamalai A., Park S.H., Kwon T.H., Pyeon M.W. and Lee M.J., *Electrochim. Acta.*, 2012; **76**: 192-200.

[10] Foletto E.L., Simões J.M., Mazutti M.A., Jahn S.L., Muller E.I., Pereira L.S.F. and Flores E.M.M., *Ceram. Int*., 2013; **39**: 4569-4574.

[11] Tuncolu I.G., Aciksari C., Suvaci E., Ozel E., Rembeza S.I., Rembeza E.S., Plotnikova E.Yu., Kosheleva N.N. and Svistova T.V., *J. Eur. Ceram. Soc*., 2015; **35**: 3885-3892.

[12] Ganbavle V.V., Patil M.A., Deshmukh H.P. and Rajpure K.Y., *J. Anal. App. Pyrol*., 2014; **107**: 233-241.

[13] Zhou Y., Li L., Zang G., Cao H. and Wang X., *J. Alloy. Compd*., 2015; **637**: 339-342.

[14] Lee W. and Lee C.H., *J. Supercrit. Fluids*, 2010; **55**: 252-258.

[15] Stambolova I., Toneva A., Blaskov V., Radev D., Tsvetanova Y., Vassilev S. and Peshev P., *J. Alloy. Compd.*, 2005; **391**: L1-L4.

[16] Wang S., Yang Z., Lu M., Zhou Y., Zhou G., Qiu Z., Wang S., Zhang H. and Zhang A., *Mater. Lett*., 2007; **61**: 3005-3008.

[17] Annamalai A., Carvalho D., Wilson K.C. and Lee M.J., *Mater. Charact*., 2010; **61**: 873-881.

[18] Ivetic T.B., Fincur N.L., Dacanin Lj.R., Abramovic B.F. and Lukic-Petrovic S.R., *Mater. Res. Bull*., 2015; **62**: 114-121.

[19] Sakurai S., Sasaki S., Okube M., Ohara H. and Toyoda T., *X-rays. Physica B*., 2008; **403**: 3589-3595.

[20] Albuquerque A.S., Ardisson J.D. and Macedo W.A.A., *J. Appl. Phys*., 2000; **87**: 4352-4357.